

## Negative Cu Ion Implantation of Insulators and In-Situ Time-Resolved Optical Spectroscopy.

Oleg A. Plaksin<sup>1,2</sup>, Hiroshi Amekura<sup>1</sup>, Kenichiro Kono<sup>1</sup>, Yoshihiko Takeda<sup>1</sup>, Takeo Suga<sup>1</sup>, Naoki Umeda<sup>3</sup> and Naoki Kishimoto<sup>1</sup>

<sup>1</sup>Nanomaterials Laboratory, National Institute for Materials Science, Tsukuba, Ibaraki 305-0003, Japan

Fax: 81-298-59-5010, e-mail: plax@mail.ru

<sup>2</sup>State Scientific Centre of Russia Federation – Institute of Physics and Power Engineering, Obninsk, 249033, Russia

<sup>3</sup>University of Tsukuba, Tsukuba, Ibaraki 305-8573, Japan

The outward mass transport during implantation of 60 keV Cu<sup>-</sup> ions in LiNbO<sub>3</sub> and Al<sub>2</sub>O<sub>3</sub> was studied by using in-situ time-resolved optical spectroscopy. Single crystals of LiNbO<sub>3</sub> and Al<sub>2</sub>O<sub>3</sub> were irradiated continuously (dose rate 20 μA/cm<sup>2</sup>) or by pulses (1 μs, repetition rate 5 kHz) of ions. Spectra of ion-induced light emission at the wavelengths from 250 to 900 nm were in-situ measured with a time resolution of 1 μs. The ratios of individual lines of the same atom species (Li for LiNbO<sub>3</sub> and Al for Al<sub>2</sub>O<sub>3</sub>) change with the dose. The change of energy distribution of sputtered atoms is explained by a competition between two mechanisms of sputtering: the sputtering induced by atomic collisions or electronic excitation. The result shows a strong relationship between irreversible structural change of implanted regions (formation of nanocomposite and damage) and energy distribution of sputtered atoms.

Key words: Ion implantation, light emission, sputtering, metal nanoparticles, insulators

### 1. INTRODUCTION

High-flux heavy-ion implantation is a powerful tool to fabricate metal nanoparticles embedded in insulators, which are promising for nonlinear optical applications [1-2]. To utilize this method, understandings of high-flux-induced kinetic processes are requisite. We focused on relationships between the ion-induced light emission (IILE) and the kinetic mass transports in fabricating Cu nanoparticles.

The IILE spectra of insulators consist of sharp lines attributed to level-to-level transitions of isolated atoms in vacuum and broad emission bands associated with electronic excitation in a solid [3-5]. Photon emission due to isolated atoms arises from an ion-induced plume off the surface. The change of intensities of atomic lines with a dose indicates changes of (1) the rate of outward mass transport, (2) the chemical composition of substrates and (3) energy distribution of sputtered atoms. In previous studies [3-5], the latter was not taken into account. In this paper, energy distributions of isolated atoms are evaluated by comparing the intensities of lines of Li (610, 675 and 812 nm) and Al (309 and 395 nm) measured during negative Cu ion implantation into LiNbO<sub>3</sub> and Al<sub>2</sub>O<sub>3</sub> respectively.

This paper is devoted to the recent progress in time-resolved optical measurement during both continuous and pulsed ion implantation. We will discuss the state-of-the-art ability to use in-situ optical measurements in fabricating metal nanoparticles.

### 2. EXPERIMENTAL

Disk-shaped specimens of LiNbO<sub>3</sub> and Al<sub>2</sub>O<sub>3</sub> single crystals were irradiated continuously, at a dose rate of 20 μA/cm<sup>2</sup>, or by pulses of negative 60 keV Cu ions. Total accumulated dose was up to 2×10<sup>17</sup> ion/cm<sup>2</sup>.

Time-resolved optical devices based on fast-response intensified CCD cameras [3] were installed into a vacuum chamber for material irradiation (Fig.1). Spectra of IILE in the wavelength range from 250 to 900 nm

were in-situ collected with a time resolution down to 1 μs. During pulsed irradiation with the pulse duration  $t_p$  of 1 μs, spectra of IILE were measured both at the moments of ion pulses and with delays.

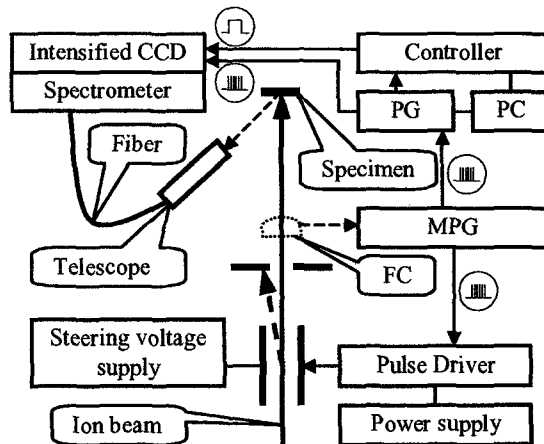


Fig.1. Schematic diagram of experiment

Frequent (5 kHz) steering the continuous ion beam produced ion pulses (Fig.1). The ion beam was initially deflected by a steering voltage and blocked by a slit plate. TTL pulses from the master pulse generator (MPG) drive a power supply and cancel the steering voltage. The same TTL pulses drive the pulse generators (PG) that gate the image intensifiers and initiate readout cycles of controllers. During a readout cycle of 0.1 to 1 s, multiple shots were accumulated on one frame of CCD. Delays were adjusted by using a signal from a Faraday cup (FC).

### 3. RESULTS AND DISCUSSION

The most prominent features of IILE of LiNbO<sub>3</sub> are Li I (Fig.2), Cu I (325 and 327 nm) and Nb I (405-412 nm)

lines, whereas Al I (Fig.2) and Cu I lines are observed for  $\text{Al}_2\text{O}_3$ . The IILE lines were attributed by using NIST Atomic Spectra Data Base.

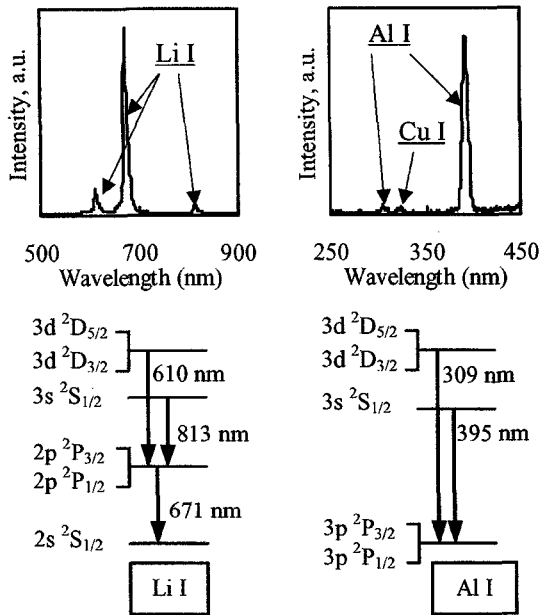


Fig.2. IILE spectra of  $\text{LiNbO}_3$  and  $\text{Al}_2\text{O}_3$  with schemes of level-to-level transitions of Li and Al atoms.

The dose dependencies of IILE lines for  $\text{LiNbO}_3$  and  $\text{Al}_2\text{O}_3$  are shown in Figs.3a and 4a respectively. As pointed out for multi-component solids [6], the intensity of atomic lines may change with a dose due to a change of chemical composition of implanted regions. No doubt, the gradual growth of Cu I lines observed during fabrication of Cu nanoparticles in various substrates (a- $\text{SiO}_2$  [5],  $\text{MgAl}_2\text{O}_4$  [3],  $\text{LiNbO}_3$  and  $\text{Al}_2\text{O}_3$ ) is due to accumulation of implants. Recently, the decrease of the ratio of Mg I to Al I line of IILE measured during Cu implantation into  $\text{MgAl}_2\text{O}_4$  was explained by formation of a magnesium-deficient layer [4]. It also seems obvious that change of the ratio of Li I to Nb I line of IILE is due to an increasing deficit of Li in the implanted region [4].

In general, the dose dependencies of IILE of  $\text{LiNbO}_3$  are qualitatively consistent with the dose dependencies of sputtering yields predicted by TRYDIN calculation. [7]. This calculation method is based on a consideration of atomic collisions in solids of variable composition, and the sputtering yields integrated over the energy of sputtered atoms are obtained. However, the proportionality between IILE intensity and integrated sputtering yield is not hold, contrary to that assumed in [3]. For example, a decrease of Al I lines of  $\text{Al}_2\text{O}_3$  is observed with increasing dose, whereas their slight increase is predicted by the calculation, assuming the proportionality mentioned. The intensities of individual lines of IILE  $I(\hbar\omega)$  may change contrariwise, probably, because the distribution of electrons over energy levels of sputtered atoms  $F(\varepsilon^*)$  depends on a differential sputtering yield  $Y(\varepsilon)$

$$I(\hbar\omega) \sim \hbar\omega F(\varepsilon^*)\dot{D},$$

$$F(\varepsilon^*) = \sum_{\varepsilon} P(\varepsilon^*, \varepsilon) Y(\varepsilon),$$

where  $\dot{D}$  is an ion flux,  $P(\varepsilon^*, \varepsilon)$  is an excitation probability,  $\varepsilon$  and  $\varepsilon^*$  are kinetic and level energies of sputtered atoms respectively.

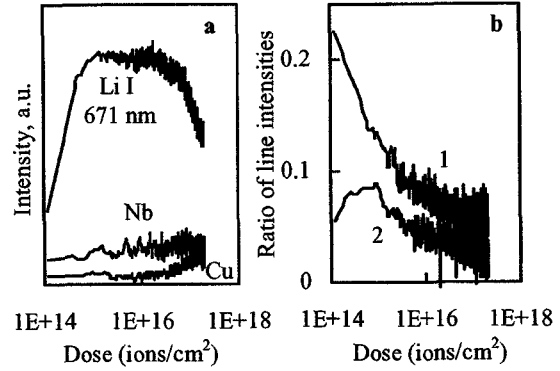


Fig.3. Intensities of IILE lines of  $\text{LiNbO}_3$  vs dose. Ratios of intensities: (1) 610 nm/671 nm; (2) 812 nm/671 nm

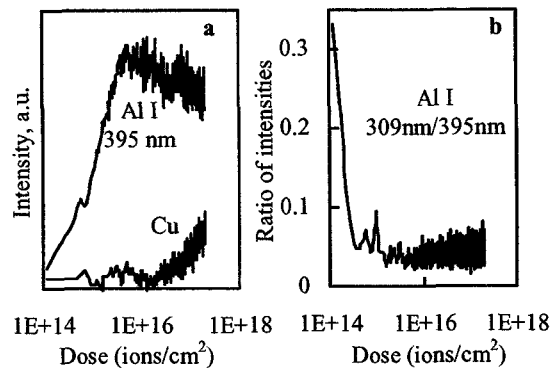


Fig.4. Intensities of IILE lines of  $\text{Al}_2\text{O}_3$  vs dose.

By comparing dose dependencies of individual lines, we investigated the processes responsible for IILE in more details. Figs.3b and 4b show that the ratios of individual lines of the same atom species (Li I for  $\text{LiNbO}_3$  and Al I for  $\text{Al}_2\text{O}_3$ ) change with a dose. That is, the change of intensity of IILE lines is partially explained by a change of differential sputtering yield or/and excitation probability of sputtered atoms. It should be noted, however, that low intensity of Al I (309 nm) line causes low accuracy of ratio.

The electron energy distribution of sputtered atoms shifts to low energies with increasing dose. After taking into account the level structures of Li and Al atoms (Fig.2), one can see that the transitions from the lowest level of excitation become more frequent as compared to other energy levels. The shift of electron energy distribution of sputtered Li atoms to low energies may be due to an increasing deficit of Li in the implanted region of  $\text{LiNbO}_3$  (increasing portion of Li atoms escaping from deep layers). However, an idea on increasing deficit of Al in  $\text{Al}_2\text{O}_3$  is not reasonable. Probably, the change of electron energy distribution is explained by a competition among various mechanisms of sputtering.

Two general mechanisms of sputtering are usually distinguished [6]: sputtering induced by either atomic collisions or electronic excitation. For these mechanisms, sputtering yield increases with increasing nuclear or electronic stopping power respectively and differs in kinetic energy distribution of sputtered atoms  $Y(\epsilon)$ .

For collision-induced sputtering, the distribution  $Y(\epsilon)$  is more broad, and the maximum of  $Y(\epsilon)$  lies at energies (few eV) slightly higher than that for ionization-induced sputtering [6, 8]. Competition between the mechanisms of sputtering may result in a shift of  $Y(\epsilon)$ . It is qualitatively consistent with our results. The maximum of dose dependence of Al I 395 nm line (energy 3.14 eV) shows that the excited state with the energy of 3.14 eV is the most probable at the dose of about  $2 \cdot 10^{15}$  ion/cm<sup>2</sup> (Fig.4a). At approximately the same dose ( $1 \times 10^{15}$  ion/cm<sup>2</sup>), the electron energy distribution of sputtered Li atoms is peaked at the energy equal to the energy of  $3s^2S_{1/2}$  state (3.37 eV), as shown in Fig.3b. With increasing dose, the maximums of these electronic distributions shift to low energies.

Two sputtering mechanisms mentioned may also differ in fast kinetics of IILE. The lifetime of IILE during collision-induced sputtering is determined by lifetimes of excited states of sputtered atoms  $\tau$  (not longer than 20 ns for Al I 395 nm line and 30 ns for Li I 671 nm line). Delay at the ballistic stage is shorter than 0.1-0.2 ns and, therefore, negligible. During ionization-induced sputtering, the situation is not so certain. For example, slow charge carrier evolution preceding the escape of atoms from a solid may affect the fast kinetics of IILE.

The decay of Li I and Al I lines measured during pulsed implantation of negative Cu ions into LiNbO<sub>3</sub> and Al<sub>2</sub>O<sub>3</sub> (Fig.5, dose  $4 \times 10^{15}$  ion/cm<sup>2</sup>) is not explained by a decay of excited states of sputtered atoms only. One microsecond after an ion pulse, the intensities of IILE lines are equal to 0.07-0.08 of their initial intensities, which is several times higher than that estimated for the decay of excited states ( $\tau/t_p = 0.02-0.03$ ).

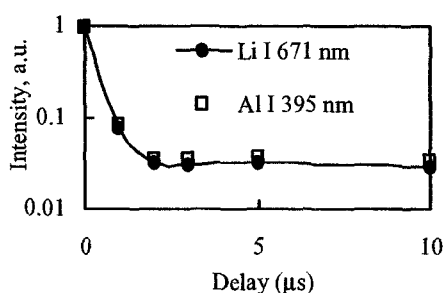


Fig.5. Decay of atomic lines of LiNbO<sub>3</sub> and Al<sub>2</sub>O<sub>3</sub> during pulsed implantation (flux  $36 \mu\text{A}/\text{cm}^2$ ).

The ratios of line intensities (Figs.3 and 4) change irreversibly with increasing dose. For example, after termination and subsequent renewal of implantation, the ratios of line intensities remain low, and further decrease with a dose is observed. Moreover, during pulsed irradiation of LiNbO<sub>3</sub>, the ratio of 610 nm to 671 nm line of Li I is of about 0.1, which is the same as that during continuous irradiation to a dose of  $4 \times 10^{15}$  ion/cm<sup>2</sup>.

Probably, the irreversible change of ratios of lines during Cu implantation into LiNbO<sub>3</sub> and Al<sub>2</sub>O<sub>3</sub> is caused by an irreversible change of structure of implanted regions. Firstly, at the dose of about  $10^{16}$  ion/cm<sup>2</sup>, all atoms of implanted region have been already involved into cascade collisions. Recently, at the same conditions, the amorphisation of Cu implanted layers of magnesium spinel and quartz has been observed by using RBS [9-10]. The severe damage of implanted regions must be accompanied by an increase of portion of weakly bound atoms, which facilitates sputtering and results in a shift of  $Y(\epsilon)$  to low energies. Secondly, at approximately the same dose a formation of nanoparticles embedded into a dielectric substrate (nanocomposite) is initiated and may affect the sputtering yield.

At present, by using IILE measurements, we cannot determine what the structural change is the most critical for IILE. In this respect, the only feature related to structure is the F<sup>+</sup>-center band of IILE of Al<sub>2</sub>O<sub>3</sub> (Fig.6). The F<sup>+</sup>-centers are associated with oxygen vacancies [11], the intensity of F<sup>+</sup>-band of IILE depending on both the oxygen vacancy concentration and the evolution of radiation-induced charge carriers (the rate of charge carrier recombination at traps) [12].

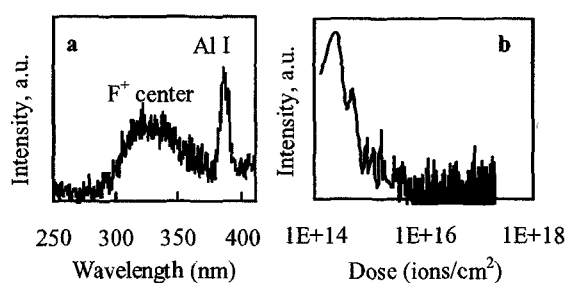


Fig.6. F<sup>+</sup>-center of Al<sub>2</sub>O<sub>3</sub>: F<sup>+</sup>-band of IILE at the onset of irradiation (a) and dose dependence of F<sup>+</sup>-band (b).

The decay of F<sup>+</sup>-band with increasing dose of Cu implantation into Al<sub>2</sub>O<sub>3</sub> is irreversible (Fig.6). It is explained as a structural change (amorphization). Due to damage of structure, it is likely that oxygen vacancies, as defects of crystal structure, almost disappear at a dose of about  $10^{16}$  ion/cm<sup>2</sup>, or charge carrier recombination takes place at the traps other than those associated with oxygen vacancies.

By using TRIM code [13], the effect of implant accumulation and nanoparticle formation on  $Y(\epsilon)$  was evaluated in frame of the mechanism of collision-induced sputtering. The nanocomposite was modeled by a layered structure (substrate/Cu/substrate) with variable both the layer thickness and Cu solute concentration in substrates. In general, a tendency opposite to that observed experimentally was obtained. The shift of  $Y(\epsilon)$  to high energies was predicted with both the increasing Cu solute concentration and the decreasing distance from the sample surface to the surface of Cu layer.

#### 4. CONCLUSION

The outward mass transport during continuous and pulsed implantation of 60 keV Cu<sup>-</sup> ions in LiNbO<sub>3</sub> and Al<sub>2</sub>O<sub>3</sub> single crystals was studied by using in-situ time-

resolved optical spectroscopy. The results on IILE are summarized as follows:

1. The intensities of atomic lines with a dose indicates changes of (1) the rate of outward mass transport, (2) the chemical composition of substrates and (3) energy distribution of sputtered atoms.
2. The ratios of individual lines of the same atom species (Li for LiNbO<sub>3</sub> and Al for Al<sub>2</sub>O<sub>3</sub>) change with the dose. The change of energy distribution of sputtered atoms is explained by a competition between two mechanisms of sputtering: the sputtering induced by atomic collisions or electronic excitation.
3. Several features of IILE during fabrication of Cu nanoparticles (dose dependence of Al line of Al<sub>2</sub>O<sub>3</sub>, change of energy distribution of sputtered atoms, decay of IILE during pulsed irradiation) are not explained in the frame of the model of sputtering based on atomic collisions.
4. The result shows a strong relationship between irreversible structural change of implanted regions (formation of nanocomposite and damage) and energy distribution of sputtered atoms.

#### ACKNOWLEDGEMENT

A part of this study was financially supported by the Budget for Nuclear Research of the MEXT, based on the screening and counseling by the Atomic Energy Commission.

#### REFERENCES

- [1] Y. Takeda, C.G. Lee, N. Kishimoto, *Nucl. Instrum. & Methods B*, 191, 422-27 (2002).
- [2] Y. Takeda, N. Umeda, V.T.Gritsyna, N. Kishimoto, *Nucl. Instrum. & Methods B*, 175-177, 463-67 (2001).
- [3] V. Bandourko, T.T. Lay, Y. Takeda, C.G. Lee, N. Kishimoto, *Nucl. Instrum. & Methods B*, 175-177, 68-73 (2001).
- [4] V.V. Bandourko, N. Umeda, N. Kishimoto, *Nucl. Instrum. & Methods B*, 190, 146-50 (2002).
- [5] N. Kishimoto, V.V. Bandourko, Y. Takeda, N. Umeda, C.G. Lee, *Nucl. Instrum. & Methods B*, 190, 207-11 (2002).
- [6] "Sputtering by particle bombardment III", Ed. by R. Behrisch, K.W. Wittmack, Springer-Verlag (1991).
- [7] TRIDYN Vs. 4.0 by W. Möller and W. Eckstein, Department of Surface Physics, Max-Planck Institute of Plasma Physics, Garching, Germany (1989).
- [8] N. Imanishi, H. Ohta, S. Ninomiya, A. Itoh, *Nucl. Instrum. & Methods B*, 164-165, 803-808 (2002).
- [9] C.G. Lee, Y. Takeda, N. Kishimoto, *Nucl. Instrum. & Methods B*, 191, 591-95 (2002).
- [10] C.G. Lee, Y. Takeda, N. Kishimoto, N. Umeda, *J. Appl. Phys.*, 90, 2195-99 (2001).
- [11] T.J. Turner, J.H. Crawford, *Phys. Rev. B*, 13, 1735-40 (1976).
- [12] O.A. Plaksin, V.A. Stepanov, *Optics and Spectroscopy*, 90/4, 542-51 (2001).
- [13] Ziegler J.F., Biersack J.P. "The Stopping and Ion Range in Solids", Pergamon Press, New York (1985).

(Received December 21, 2002; Accepted March 26, 2003)